

# **Adsorption of Rhodamine B from an Aqueous Solution: Kinetic, Equilibrium and Thermodynamic Studies**

M.Santhi<sup>1</sup>, P.E.Kumar<sup>2\*</sup>

Assistant Professor, PG and Research, Department of Chemistry, Erode Arts and Science College (Autonomous),  
Erode, Tamil Nadu, India<sup>1</sup>.

Associate Professor, PG and Research Department of Chemistry, Erode Arts and Science College (Autonomous),  
Erode, Tamil Nadu, India<sup>2</sup>.

\* Corresponding Author

**ABSTRACT:** Activated carbon was developed from *Typha Angustata L.*, characterized and used for the removal of Rhodamine B from waste water successfully. Rhodamine B is one of the water soluble, basic red cationic Xanthene class dyes, a common water tracer fluorescent. Batch adsorption experiments were carried out as a function of  $P^H$ , contact time, initial concentration of the adsorbate, adsorbent dosage and temperature. The experimental data were analyzed using the pseudo second order kinetic model. The equilibrium data satisfied by Langmuir Isotherm models. The changes in standard free energy ( $\Delta G^\circ$ ), Standard Entropy ( $\Delta S^\circ$ ) Standard enthalpy ( $\Delta H^\circ$ ) were calculated. The thermodynamic study has showed that the dye adsorption phenomenon onto AC-MnO<sub>2</sub>-NC was favorable, endothermic and spontaneous.

**KEYWORDS:** AC-MnO<sub>2</sub>-NC, Rhodamine-B, Adsorption isotherm, Kinetics, Equilibrium.

## **I. INTRODUCTION**

Among the different pollutants of aquatic ecosystem, dyes are a large and important group of industrial chemicals for which world production in 1978 was estimated at 640,000 tons[1]. Dyes are widely used in industries such as textiles, rubber, paper, plastic, cosmetics, etc to color their products. The dyes are invariably left as the major waste in these industries.

Synthetic dyes are used extensively in many industries including dye houses, paper prints and textile dyers. A significant proportion of synthetic dyes are lost annually to waste streams during textile processing, which eventually enters the environment [2]. Some of dyes are toxic and carcinogenic and require separation and advanced treatment of textile effluents before discharge into conventional systems [3]. Due to biodegradability of dyes, a conventional biological waste water treatment process is not very efficient in treating dye waste water.

The removal of color from waste water can be accomplished by flotation, chemical coagulation, chemical oxidation and adsorption [4]. Hence investigations have been conducted on physicochemical methods of removing color from textile effluents [5].

These studies include chemical oxidation [6], membrane filtration [7] and adsorption techniques [8]. In these techniques adsorption has been found to be an efficient process to remove dye. Activated carbon [9] and natural adsorbents such as banana and orange peel [10], apple pomace and wheat straw [11], waste mud [12], wood materials [13], Jambonut [14] and *Borassus flabellifer L.* [15] have been extensively used as adsorbents. Activated carbon adsorption has been found to be an effective means of waste water treatment.

# International Journal of Innovative Research in Science, Engineering and Technology

(An ISO 3297: 2007 Certified Organization)

Vol. 4, Issue 2, February 2015

Adsorption hold promise in the treatment of waste water as it is inexpensive simply designed, easy to handle. The aim of this study was to use the dried AC-MnO<sub>2</sub>-NC to remove one important reactive dye, RhodamineB (RhB) from aqueous solution. RhodamineB(RhB)is one of the water soluble xanthene class dyes, a basic red cationic dye which is a common water tracer fluorescent. It is often used textile and food industries.

## II. MATERIALS AND METHODS

### 2.1 Adsorbate

Basic dye used in this study is Rhodamine B purchased from S.d. fine chemicals, Mumbai, India. RhB has molecular formula-C<sub>28</sub>H<sub>31</sub>ClN<sub>2</sub>O<sub>3</sub>.The dye concentration in supernatant solution was determined at characteristic wavelength [ $\lambda_{max}$  =543nm] by double beam UV-visible spectrophotometer [Systronics 2202].

### 2.2. Preparation of Activated Carbon

The TyphaAngustata L plant materials were collected from local area situated at Thindal, Erode District, Tamilnadu. They were cut into small pieces and dried for 20 days. Finally it was taken in a steel vessel and heated in muffle furnace. The temperature was raised gradually upto 500<sup>o</sup>c and kept it for half an hour. The carbonised material was ground well and sieved to different particle size. It was stored in a plastic container for further studies. In this study particle size of 0.15 to 0.25mm was used.

### 2.3. Preparation of AC-MnO<sub>2</sub>-NC

Activated Carbon [3gm] was allowed to swell in 15mL of water-free Alcohol and stirred for 2 hours at 25<sup>o</sup>C to get uniform suspension. At the same time, the Manganese dioxide [3gm] was dispersed into water-free Alcohol [15mL]. Then the diluted Manganese dioxide was slowly added into the suspension of activated Carbon and stirred for a further 5 hours at 25<sup>o</sup>C.To this, 5mL alcohol and 0.2mL of deionised water was slowly added. The stirring was continued for another 5 hours at 25<sup>o</sup>C and the resulting suspension was kept overnight in a vacuum oven for 6 hours at 80<sup>o</sup>C. Characteristics of the AC-MnO<sub>2</sub>-NC were determined and the results are summarized in Table.1.

**Table.1. Physical and Chemical Properties of Adsorbents**

Physical and Chemical Properties	AC-MnO <sub>2</sub> -NC
[1]. Moisture content [%]	9.19
[2]. Volatile matter [%]	62.73
[3]. Ash [%]	17.15

### 2.3 Characterisation of Adsorbent

Physico-Chemical characteristics of the adsorbents were studied as per the standard testing methods [16]. Figure 1, 2 shows the XRD pattern of pure AC and AC-MnO<sub>2</sub>-NC respectively. The peaks at 28° [Figure 1] and at 30° [Figure 2] confirm the presence of AC-MnO<sub>2</sub> phase in the nanocomposite. The surface morphology of the adsorbent was visualized via scanning electron microscopy [SEM] are shown in Figure 3 and 4. The diameter of the composite range was 10µm. FTIR spectra indicate the presence of MnO<sub>2</sub> peak at 430cm<sup>-1</sup>.

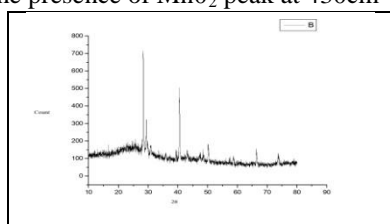


**Figure 1. XRD analysis of Activated Carbon**

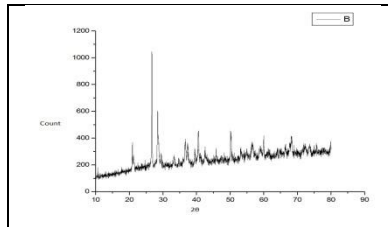


**Figure 2. XRD analysis of AC-MnO<sub>2</sub>-NC**

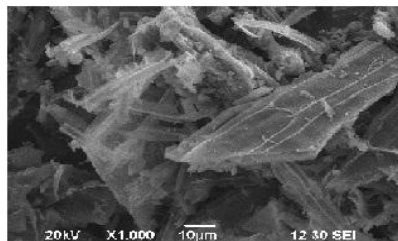


**Figure 3. SEM of Activated Carbon**

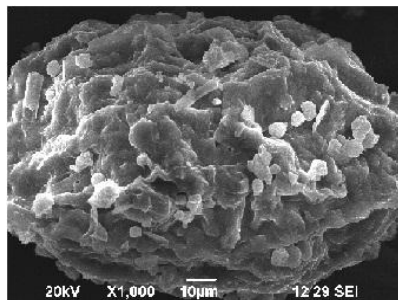


**Figure 4. SEM of AC-MnO<sub>2</sub>-NC**

**2.4 Batch adsorption method**

A stock solution [1000mg/L] of RhB was prepared by dissolving an appropriate amount of each dye in double distilled water, which was diluted to desired concentrations of 10, 20, 30 and 40mg/L. Batch adsorption [17] experiments were carried out to investigate the effect of P<sup>H</sup>, temperature, adsorbent dose, initial dye concentration, contact time on the adsorption of RhB on AC-MnO<sub>2</sub>-NC by varying the parameters under study and keeping other parameters constant. In each experiment pre weighed amount of adsorbent was added to 50mL of dye solution taken in a 150mL of conical flask and the pH was adjusted by using 0.1M NaOH or 0.1M HCL. The resulting solution was agitated at 200rpm on a stirrer at constant temperature and centrifuged [Remi Research Centrifuge].

The percentage removal of dye and amount of dye adsorbed on AC-MnO<sub>2</sub>-NC was calculated by equation [1] and equation [2] respectively.

$$\% \text{ removal} = \frac{100[C_0 - C_e]}{C_e} \text{-----} > [1]$$

$$q_e = \frac{[C_0 - C_e] V}{W} \text{-----} > [2]$$

# International Journal of Innovative Research in Science, Engineering and Technology

(An ISO 3297: 2007 Certified Organization)

Vol. 4, Issue 2, February 2015

Where  $q_e$  is the quantity of dye adsorbed on the adsorbent at the time of equilibrium [mg/g],  $C_o$  and  $C_e$  are the initial and equilibrium concentrations [ $\text{mgL}^{-1}$ ] of the dye in solution respectively,  $V$  is the volume [L] of solution and  $W$  is the weight of adsorbent [g]. All adsorption experiments were performed in triplicate and the mean values were used in data analysis.

### 2.5. Batch Kinetic Studies

The batch kinetic [17] experiments were basically identical to these of adsorption equilibrium method. The amount of adsorption  $q_t$  [mg/g] at time  $t$ , was calculated by,

$$q_t = \frac{[C_o - C_t]V}{W} \quad \text{-----> [3]}$$

Where  $C_t$  [mg/L] is the liquid phase concentration of dye at any time.

## III. THEORY OF ADSORPTION ISOTHERM

To quantify the adsorption capacity of the adsorbent for the removal of dyes, the most commonly used isotherm, namely Freundlich, Langmuir and Tempkin have been adopted.

### 3.1. Freundlich Isotherm

The linear form of Freundlich isotherm [18] is represented by the equation.

$$\log q_e = \log k_f + 1/n \log C_e \quad \text{-----> [4]}$$

Where  $q_e$  is the amount of dyes absorbed per unit weight of the adsorbent, [mg/L],  $k_f$  is [mg/g [L/mg]] measures of adsorption capacity and  $1/n$  is the adsorption intensity. In general  $k_f$  Value increases the adsorption capacity for a given adsorbate increases. The magnitude of the exponent  $1/n$  gives an indication of the favorability of adsorption. The value of  $n > 1$  represents favorable adsorption condition [19,20] or the value of  $1/n$  are lying in the range of 1 to 10 confirms the favorable condition for adsorption. The linear plot of  $\log q_e$  Vs  $\log C_e$  shows that the adsorption obeys the Freundlich model.

### 3.2. Langmuir Isotherm

Langmuir isotherm model [21] is based on the assumption that maximum adsorption corresponds to a saturated monolayer of solute molecules on the adsorbent surface. The linear form of the Langmuir isotherm equation can be described by

$$C_e / q_e = \frac{1}{Q_o K_L} + \frac{C_e}{Q_o} \quad \text{-----> [5]}$$

Where  $C_e$  [mg/L] is the equilibrium concentration of the adsorbate,  $q_e$  [mg/g] is the amount of adsorbate adsorbed per unit mass of adsorbent,  $Q_o$  and  $K_L$  are Langmuir constants related to adsorption capacity and rate of adsorption respectively.  $Q_o$  is the amount of adsorbate at complete monolayer coverage [mg/g] which gives the maximum adsorption capacity of the adsorbent and  $K_L$  [L/mg] is the Langmuir isotherm constant that relates to the energy of adsorption [or rate of adsorption]. The linear plot of specific adsorption capacity  $C_e/q_e$  against the equilibrium concentration  $C_e$  shows that the adsorption obeys the Langmuir model. The Langmuir constant  $Q_o$  and  $K_L$  were determined from the slope and intercept of the plot and are presented in Table 2. In order to find out the feasibility of the isotherm, the essential characteristics of the Langmuir isotherm can be expressed in terms of dimensionless constant separation factor  $R_L$  [22, 23] by the equation,

$$R_L = \frac{1}{1 + K_L C_o} \quad \text{-----> [6]}$$

# International Journal of Innovative Research in Science, Engineering and Technology

(An ISO 3297: 2007 Certified Organization)

Vol. 4, Issue 2, February 2015

Where  $C_0$  [mg/L] is the initial concentration of adsorbate and  $K_L$  [L/mg] is Langmuir isotherm constant. The parameter  $R_L$  indicate the nature of the adsorption isotherm.

$R_L > 1$	Unfavorable adsorption
$0 < R_L < 1$	Favorable adsorption
$R_L = 0$	Irreversible adsorption
$R_L = 1$	Linear adsorption

The  $R_L$  values lies between 0 to 1 indicate the process is favorable adsorption.

### 3.3. Tempkin isotherm

Tempkin isotherm contains a factor that explicitly takes into account adsorbing species-adsorbate interactions. This isotherm assumes that : [1]. The heat of adsorption of all the molecules in the layer decreases linearly with coverage due to adsorbate-adsorbate interactions, and [2] Adsorption is characterized by a uniform distribution of binding energies, up to some maximum binding energy [24].

Tempkin isotherm is represented by the following equation:

$$q_e = \frac{RT}{b} \ln[AC_e] \text{ -----} > [7]$$

equation [7] can be expressed in its linear form as:

$$\begin{aligned} q_e &= \frac{RT}{b} \ln A + \frac{RT}{b} \ln C_e \\ q_e &= B \ln A + B \ln C_e \text{ -----} > [8] \end{aligned}$$

Where  $B = RT/b$

The adsorption data can be analysed according to equation [8]. A plot of  $q_e$  Versus  $\ln C_e$  enables the determination of the isotherm constants A and B. A is the equilibrium binding constant [1/mol] corresponding to the maximum binding energy and constant B is related to the heat of adsorption. For RhB adsorption by AC-MnO<sub>2</sub>-NC and values of the parameters are given in Table [2].

## IV. ADSORPTION KINETICS

The study of adsorption kinetics describes the solute uptake rate and evidently this rate controls the residence time of adsorbate uptake at the Solid-Solution interface. The kinetics of RhB adsorption by the AC-MnO<sub>2</sub>-NC were analysed using Pseudo first-order, Pseudo second – order, Elovich and intra particle diffusion model. The conformity between experimental data and the kinetic models was expressed by the correlation co-efficient [ $R^2$ ] value, the  $R^2$  values close or equal to 1. A relatively high  $R^2$  value indicates that the model successfully describes the kinetics of RhB dye adsorption.

### 4.1. Pseudo first order kinetic model

The linear form of Langergren's first order rate equation is as follows [25],

$$\ln [q_e - q_t] = \ln q_e - K_1 t \text{ -----} > [9]$$

Where  $q_e$  is the amount of dye adsorbed onto the adsorbent at equilibrium [mg/g],  $q_t$  is the amount of dye adsorbed on to the adsorbent at any time t [mg/g] and  $K_1$  [ $\text{min}^{-1}$ ] is rate constant of the pseudo first order adsorption which can be calculated from the slope of the linear plot of  $\ln[q_e - q_t]$  Vs t [slope =  $K_1$ ,  $q_e$  = intercept]. The adsorption of pseudo first order rate constant and correlation coefficient [ $R^2$ ] values are summarized in Table [3].

### 4.2 Pseudo second order kinetic model

The linearised form of the pseudo second order model as given by Ho [26] is

$$t/q_t = 1/K_2 q_e^2 + t/q_e \text{ -----} > [10]$$

Where  $K_2$  [ $\text{gmg}^{-1} \text{min}^{-1}$ ] is the rate constant of the pseudo second order adsorption,  $q_e$  is the amount of dye adsorbed on the adsorbent at equilibrium [mg/g], and  $q_t$  is the amount of dye adsorbed on the adsorbent at any time, t [mg/g]. The plot of  $t/q_t$  Vs t should give a linear relationship from which  $q_e$  and  $K_2$  can be determined from the slope and intercept

# International Journal of Innovative Research in Science, Engineering and Technology

(An ISO 3297: 2007 Certified Organization)

Vol. 4, Issue 2, February 2015

of the plot respectively. The pseudo second order rate constant  $K_2$ , the correlation coefficient  $[R^2]$  values are summarized in Table [3].

### 4.3. Elovich model

The elovich model equation is generally expressed as [27]

$$q_t = 1/\beta \ln[\alpha\beta] + 1/\beta \ln t \text{ -----} > [11]$$

Where  $\alpha$ - is the initial adsorption rate  $[mg\ g^{-1}\ min^{-1}]$ ,  $\beta$  is the desorption constant  $[gmg^{-1}]$  during any one experiments. A plot of  $q_t$  Vs  $\ln t$  should yield a linear relationship with a slope of  $[1/\beta]$  and an intercept of  $1/\beta \ln[\alpha\beta]$ . The elovich model parameters  $\alpha$ ,  $\beta$  and correlation coefficient  $[R^2]$  are summarized in Table [3].

### 4.4. Intraparticle diffusion model

The intraparticle diffusion model used here refers to the theory proposed by Weber and Morris [28] based on the following equation for the rate constant

$$q_t = K_{id} t^{1/2} + C \text{ -----} > [12]$$

Where  $K_{id}$  is the intraparticle diffusion rate constant  $[mg\ g^{-1}\ min^{-1/2}]$  and C is constant. If the rate limiting step is intraparticle diffusion, the graphical representation of adsorbed dye  $q_t$   $[mgg^{-1}]$  depending on the square root of the contact time  $[t^{1/2}]$  should yield a straight line passing through the origin [40]. The plot of  $q_t$  Vs  $t^{1/2}$  will give the value of the intraparticle diffusion rate constant  $[K_{id}]$  and correlation coefficient  $[R^2]$  can be determined from the slope respectively. The intraparticle diffusion rate constant  $K_{id}$ , the correlation co-efficient  $[R^2]$  values are summarized in Table [3].

## V. THERMODYNAMIC TREATMENT OF THE ADSORPTION PROCESS

The effect of temperature on the adsorption of RhB by AC-MnO<sub>2</sub>-NC adsorbents were investigated at 303, 313, 323 and 333K. Thermodynamic parameters, such as change in enthalpy  $[\Delta H^\circ]$ , entropy  $[\Delta S^\circ]$  and Gibb's free energy  $[\Delta G^\circ]$  were determined for the MG by AC-MnO<sub>2</sub>-NC using equation [13] & [14]. [29].

$$\ln [q_e m / C_e] = \Delta S^\circ / R - \Delta H^\circ / RT \text{ -----} > [13]$$

$$\Delta G^\circ = \Delta H^\circ - T \Delta S^\circ \text{ -----} > [14]$$

Where m is the adsorbent dose  $[mg/L]$ ,  $C_e$  is the equilibrium concentration  $[mg/L]$  of the dye in solution and  $q_e m$  is the solid-phase concentration  $[mg/L]$  at equilibrium. R is the gas constant  $[8.314J/mole/K]$  and T is the temperature  $[K]$ .  $\Delta H^\circ$ ,  $\Delta S^\circ$  and  $\Delta G^\circ$  are changes in enthalpy  $[KJ/mol]$ , entropy  $[J/mol/K]$  and Gibb's free energy  $[KJ/mol]$  respectively.

The values of  $\Delta H^\circ$  and  $\Delta S^\circ$  were determined from the slope  $[-\Delta H^\circ/R]$  and the intercept  $[\Delta S^\circ/R]$  of the plots of  $\ln [q_e m / C_e]$  Vs  $1/T$ . The  $\Delta G^\circ$  values were calculated by using equation [14]. The values of the thermodynamics parameters are presented in Table [4].

## VI. RESULTS AND DISCUSSIONS

### 6.1. Effect of Agitation time Vs initial dye concentration

Effect of Agitation time Vs initial dye concentration  $[10, 20, 30$  and  $40\ mg/L]$  on removal of RhB by AC-MnO<sub>2</sub>-NC are shown in Figure 5. The percent removal of RhB increased with increase in agitation time and reached equilibrium at 210min. The percent dye removal at equilibrium decreased from 78.23 to 99.23 as the dye concentration was increased from 10 to 40 mg/L. It is clear that the removal of dye depends on the initial concentration of the dye. The removal curves are single, smooth and continuous leading to saturation.

# International Journal of Innovative Research in Science, Engineering and Technology

(An ISO 3297: 2007 Certified Organization)

Vol. 4, Issue 2, February 2015

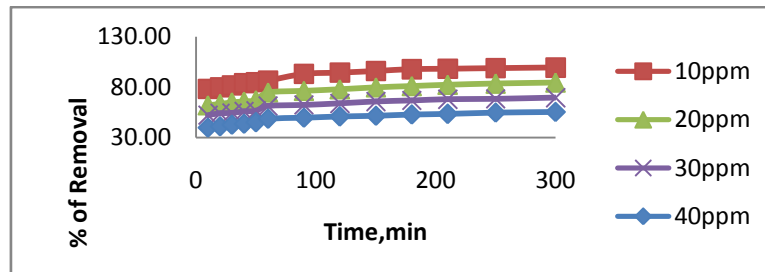


Figure 5. Effect of Agitation Time Vs initial concentration of RhB by AC – MnO<sub>2</sub>-NC

### 6.2. Effect of adsorbent dosage

The removal of RhB by AC – MnO<sub>2</sub>-NC at different adsorbent dosage are shown in Figure.6. [10mg to 600mg/50mL] was tested for the dye concentrations 10, 20, 30 and 40mg/L. The adsorption increases with increase in adsorbent concentration; this is due to the increase in surface area and availability of more adsorption site. The percentage removal of RhB is greatly increases in the range of 10-600mg/50mL after that small change occur. So the optimum adsorbent carbon dosages for the experiments were carried out using 100mg/50mL.

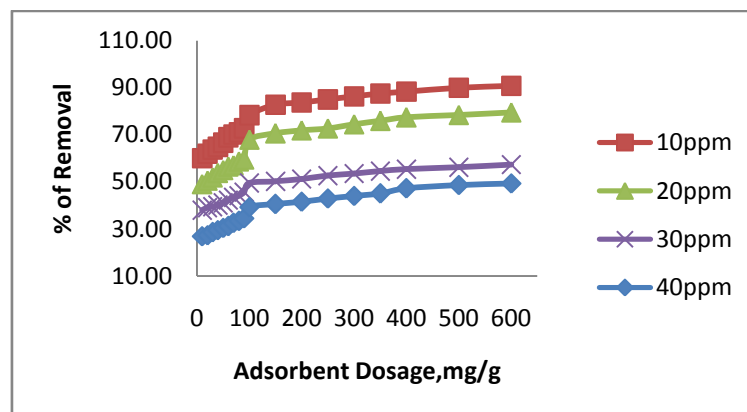


Figure 6. Effect of Adsorbent Dosage of RhB by AC-MnO<sub>2</sub>-NC

### 6.3. Effect of pH

Effects of pH on the removal of RhB by AC-MnO<sub>2</sub>-NC are shown in Figure.7. The solution pH is one of the most important factors that control the adsorption of RhB on the adsorbent material. Therefore an increase in pH may cause an increase [or] decrease in the adsorption capacity. The adsorption capacity can be attributed to the chemical form of RhB in a solution at the specific pH [or] due to different functional group on the adsorbent surface. To examine the effect of pH on the percentage removal of RhB gradually increases as the pH increases. The pH value up to 8.95 the percentage removal is up to 59.32 after that suddenly increases. At that solution pH the adsorbent surface negatively charged and favors uptake of cationic dyes due to increased electrostatic force of attraction. Therefore, all the experiments were carried out at the pH 8.95. For 40mg/L dye concentration the percent removal increased from 34.46 to 64.76 when the pH was increased from 2 to 14 and the percent removal remained almost the same above pH 9.

# International Journal of Innovative Research in Science, Engineering and Technology

(An ISO 3297: 2007 Certified Organization)

Vol. 4, Issue 2, February 2015

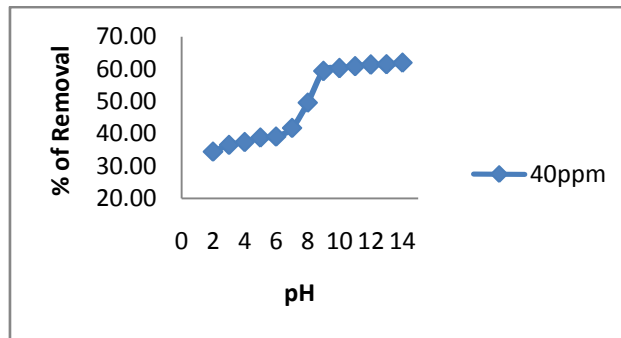


Figure 7. Effect of pH of RhB by AC-MnO2-NC

### 6.4. Effect of Temperature

The effect of temperature of adsorption of RhB are presented in Figure 8. For concentration 40 mg/L adsorbent was carried out at 30°, 40°, 50° and 60°C. The percent removal of dye increased from 20.04 to 77.73. This indicates that increase in adsorption with increase in temperature may be due to increase in the mobility of the large dye ions. Moreover, increasing temperature may produce a swelling effect within the internal structure of the adsorbent, penetrating the large dye molecule further.

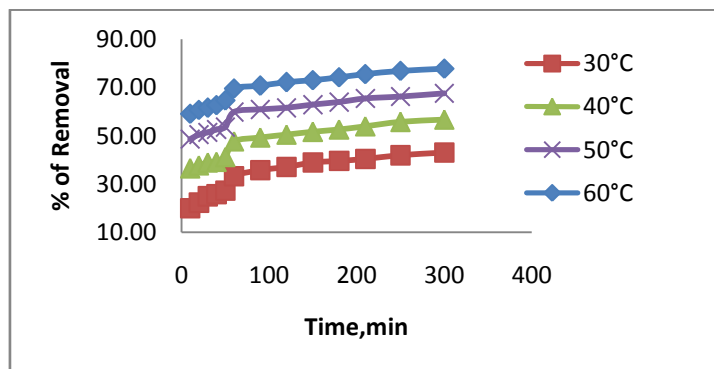


Figure 8. Effect of Temperature of RhB by AC-MnO2-NC

### 6.5. Adsorption isotherms

Three different isotherm models were used to fit the experimental data the Langmuir, Freundlich and Tempkin models are given in Figure. 9, 10 and 11 and the parameter values are given in the Table 2.

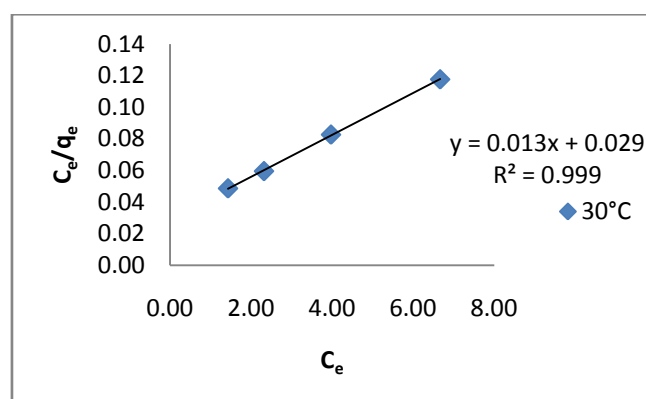


Figure 9. Plot of Langmuir isotherm

## International Journal of Innovative Research in Science, Engineering and Technology

(An ISO 3297: 2007 Certified Organization)

Vol. 4, Issue 2, February 2015

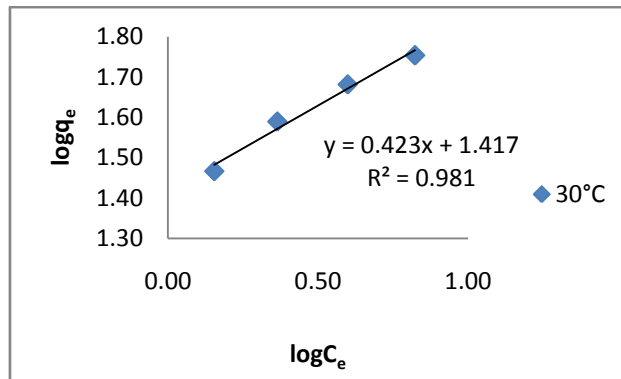


Figure 10. Plot of Freundlich isotherm

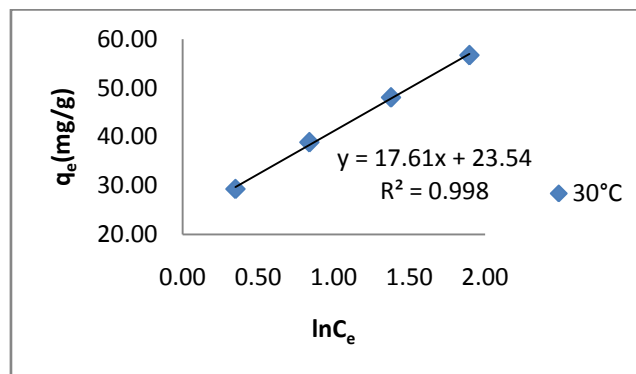


Figure 11. Plot of Tempkin isotherm

**Table.2. Langmuir, Freundlich and Tempkin isotherm parameter for adsorption of RhB by AC-MnO<sub>2</sub>-NC adsorbent**

Initial dye concentration mg/L	Langmuir				Freundlich			Tempkin			
	Q <sub>0</sub> [mg/g]	K <sub>L</sub> [L/g]	R <sup>2</sup>	R <sub>L</sub>	K <sub>f</sub> [mg/g/[L/g]]	n	R <sup>2</sup>	A	b	B	R <sup>2</sup>
60	76.923	2.230	0.999	0.0074	26.121	2.364	0.981	3.8064	140.69	17.61	0.998
80				0.0057							
100				0.0044							
120				0.0037							

From the Table.2, it is clear that, the Langmuir isotherm constant value indicate the adsorption capacity Q<sub>0</sub> = 76.923 mg/g. The Langmuir isotherm can also be expressed in terms of a dimensionless constant separation factor [R<sub>L</sub>]. The R<sub>L</sub> Value lies in between 0 to 1 indicate the adsorption is favorable for all the initial dye concentration.

# International Journal of Innovative Research in Science, Engineering and Technology

(An ISO 3297: 2007 Certified Organization)

Vol. 4, Issue 2, February 2015

From the Table.2, it is clear that, the Freundlich isotherm constant value indicate  $1/n$  [or]  $n$  is the adsorption intensity. The 'n' values lies in between 1 to 10 confirm the favorable condition for adsorption.

From the table.1, it is clear that, the Tempkin isotherm constant value indicate maximum binding energy  $B=17.61$  and it is related to the heat of adsorption.

All the three models explain correlation co-efficient  $[R^2]$ . From Table.2, RhB on AC-MnO<sub>2</sub>-NC to fit Langmuir model. This indicates monolayer adsorption.

### 6.6. Adsorption Kinetics

The kinetics of MG dye adsorption on RhB by AC-MnO<sub>2</sub>-NC was studied with respect to different initial concentration. For evaluating the adsorption kinetics of RhB, the Pseudo first order, the pseudo second order, Elovich model and intraparticle diffusion model were used to fit the experimental data by using linear regression analysis method and it is given in Figure.12, 13, 14 and 15. The parameters of this model are summarized in Table.3. The high correlation coefficient  $[R^2]$  values indicate the fitness of the model.

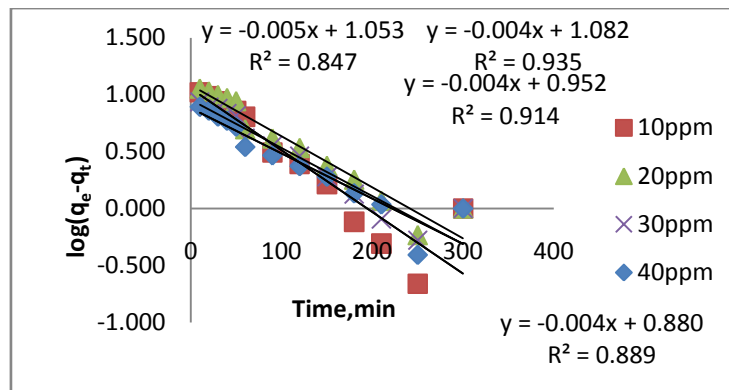


**Figure.12 Pseudo first order kinetic model**

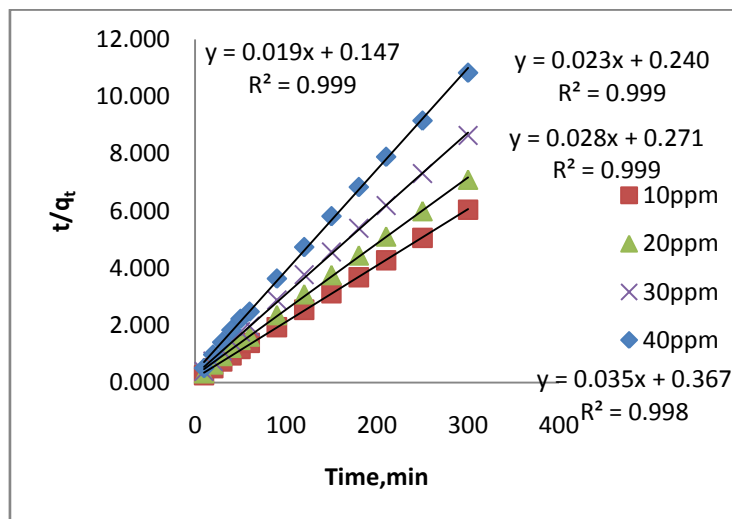


**Figure.13 Pseudo second order kinetic model**

## International Journal of Innovative Research in Science, Engineering and Technology

(An ISO 3297: 2007 Certified Organization)

Vol. 4, Issue 2, February 2015

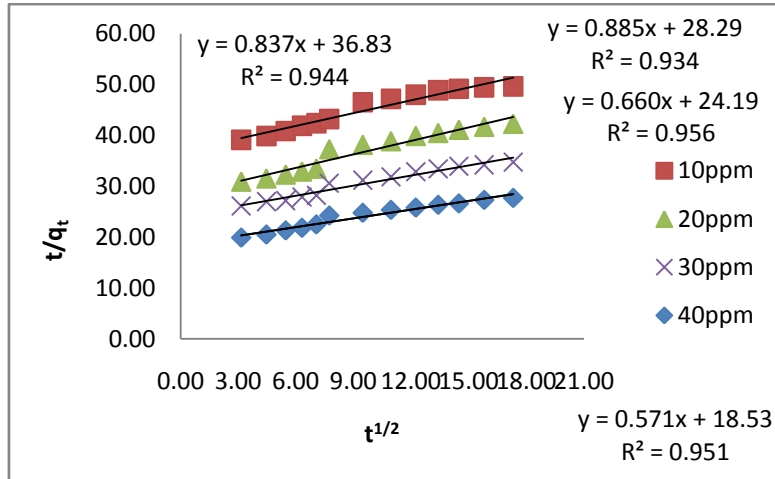


Figure.14 Intraparticle diffusion model

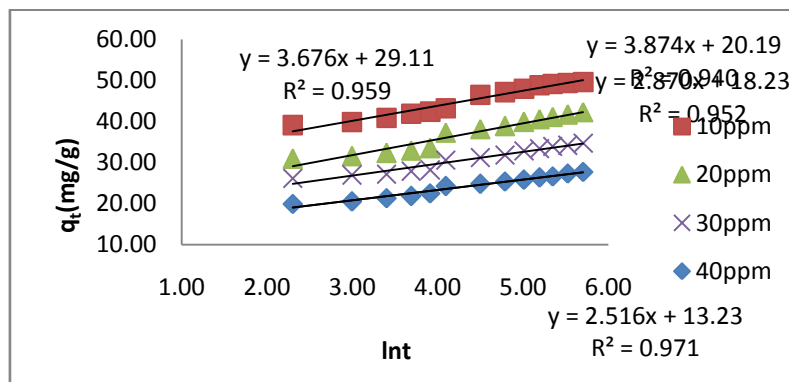


Figure.15 Elovich model

Table.3. The kinetic parameter for the adsorption of RhB by AC-MnO<sub>2</sub>-NC adsorbent.

Initial dye concentration	Pseudo first order				Pseudo second order				Intraparticle diffusion			Elovich		
	q <sub>e,exp</sub>	q <sub>e,cal</sub>	K <sub>1</sub>	R <sup>2</sup>	q <sub>e,exp</sub>	q <sub>e,cal</sub>	K <sub>2</sub>	R <sup>2</sup>	K <sub>id</sub>	C	R <sup>2</sup>	α	β	R <sup>2</sup>
10	99.23	11.2979	1.151 x 10 <sup>-2</sup>	0.847	99.23	52.631	2.455 x 10 <sup>-3</sup>	0.999	0.837	36.83	0.918	10197.521	0.2724	0.959
20	84.57	12.0781	9.212 x 10 <sup>-3</sup>	0.935	84.57	43.478	2.204 x 10 <sup>-3</sup>	0.999	0.885	28.29	0.929	710.09	0.2581	0.940
30	69.47	8.9536	9.212 x 10 <sup>-3</sup>	0.914	69.47	35.714	2.893 x 10 <sup>-3</sup>	0.999	0.660	24.19	0.957	1645.336	0.3484	0.952
40	55.40	7.5857	9.212 x 10 <sup>-3</sup>	0.889	55.40	28.571	3.337 x 10 <sup>-3</sup>	0.998	0.571	18.53	0.937	483.185	0.3974	0.971

# International Journal of Innovative Research in Science, Engineering and Technology

(An ISO 3297: 2007 Certified Organization)

Vol. 4, Issue 2, February 2015

From the kinetic data, the  $q_e$  value calculated from the pseudo first order model is less than that of the experimental value. But the  $q_e$  values calculated from the pseudo second order model are nearly equal to the experimental value. The correlation co-efficient [ $R^2$ ] is high for pseudo second order. So that the adsorption of RhB by AC-  $MnO_2$ -NC is to follow the pseudo second order kinetic model.

The experimental data were used for intraparticle diffusion model, the intraparticle diffusion constant [ $K_{id}$ ], intercept and the correlation co-efficient [ $R^2$ ] are calculated. From these data the intercept value indicates that the lines are not passing through origin, therefore some other process that may affect the adsorption. The correlation co-efficient [ $R^2$ ] is value is less than that of pseudo second order model.

The same experimental data were used for Elovich model, the initial adsorption rate [ $\alpha$ ], desorption constant [ $\beta$ ] and the correlation co-efficient [ $R^2$ ] are calculated. But, the correlation Co-efficient [ $R^2$ ] is less than that of pseudo second order model.

Finally, From Table.3 indicates all these four kinetic models, RhB by AC-  $MnO_2$ -NC is to follow pseudo second order kinetic model.

### 6.7. Thermodynamic parameter

The Thermodynamic parameters for the adsorption process of RhB by AC- $MnO_2$ -NC are the changes in standard free energy change [ $\Delta G^0$ ], standard enthalpy change [ $\Delta H^0$ ] and standard entropy change [ $\Delta S^0$ ] and is shown in Fig.16. The values of these parameters were calculated and are shown in Table.3

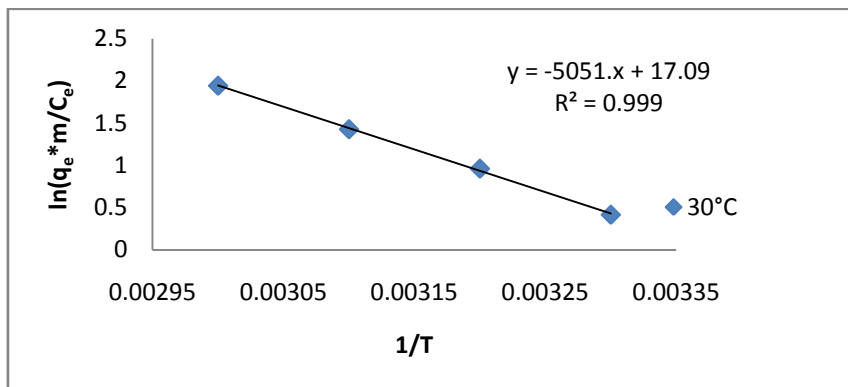


**Fig.16. Thermodynamic parameter**

**Table.4. Thermodynamic parameter values of RhB by AC- $MnO_2$ -NC**

$\Delta G^0$ [kJ/mol]				$\Delta S^0$ [J/mol/K]	$\Delta H^0$ [kJ/ mol]
303K	313K	323 K	333 K	142.0862	41.9940
-43.0101	-44.4309	-45.8518	-47.2727		

## International Journal of Innovative Research in Science, Engineering and Technology

(An ISO 3297: 2007 Certified Organization)

Vol. 4, Issue 2, February 2015

The adsorption data indicates that  $\Delta G^\circ$  values were negative at all temperatures. The negative  $\Delta G^\circ$  confirms the spontaneous nature of adsorption of RhB by AC-MnO<sub>2</sub>-NC. The magnitude of  $\Delta G^\circ$  suggests that adsorption is physical adsorption process. The positive value of  $\Delta H^\circ$  were further confirms the endothermic nature of adsorption process. The positive  $\Delta S^\circ$  showed increased randomness at the solid – solution interface during the adsorption of RhB by AC-MnO<sub>2</sub>-NC adsorbent.

### VII. DESORPTION STUDIES

After activated carbon is saturated with dye molecules, different solvents could be used to regenerate the activated carbon to restore its dye adsorptive capability [30]. Desorption with acetic acid revealed that the regeneration of adsorbent was satisfactory, which confirms the physisorptive nature of adsorption.

### VIII. CONCLUSIONS

The present study shows that AC-MnO<sub>2</sub>-NC is an effective adsorbent for the removal of RhB from aqueous solution. Adsorption followed the Langmuir isotherms. The adsorption capacity was found to be 76.923 mgg<sup>-1</sup>. The thermodynamic parameters were found to be thermodynamically favourable physical adsorption process. Evaluation of thermodynamic parameters showed the process as endothermic and spontaneous. The kinetic parameters fit for Pseudo second order model. Desorption studies reveals that satisfactory desorption taking place confirming physisorptive nature of adsorption. Complete removal of the dye can be achieved using an appropriate dosage of the adsorbent and pH for waste waters. The results would be useful for the fabrication and designing of waste water treatment plants for the removal of dye. Since the raw material is freely available in large quantities the treatment method, seems to be economical.

### REFERENCES

- [1] Clarke, E.A., Anliker, R., Organic dyes and pigments., in the Handbook of Environmental chemistry part A. Anthropogenic compounds. Hutzinger.O.(Ed). Springer – Verlag, Heidelberg, vol.3, pp.181 -215, 1980.
- [2] Hu, T.L., Removal of reactive dyes from aqueous solution by different bacterial genera, Wat.Sci.Technol, vol. 34, pp. 89-95, 1996.
- [3] Brown, M.A., Crit, Predicting azo dye Toxicity, Rev.Envirion. Sci. Technol, vol.23, pp.24, 1993.
- [4] Zhou, W, Zimmermann,W, Decolourisation of industrial effluents containing reactive dyes by actinomycetes, FEMS Microbiol,Lett,vol.107, pp.157 -16, 1993.
- [5] Banat, I.M., Nigam, P., Singh D., and Marchent,R., Microbial decolourisation of textile –dye containing effluent,Bioresource Technol, vol, 58,pp. 217 – 227, 1996.
- [6] Arslon, I., Balcioglu I.A., and Bahnemann, D.W.,Advanced chemical oxidation of reactive dyes in simulated dyehouse effluents of ferrioxalate-Fenton/UV-A and TiO<sub>2</sub>/UV-A Processes, Dyes Pigments,vol, 47, pp, 207-218, 2000.
- [7] Purkait, M.K., Dasgupta S., and De,S., Removal of dye from waste water using micellar enhanced ultrafiltration and recovery of surfactant,Sep.purif.Technol, vol,37, pp. 81-92, 2004.
- [8] Garg, V.K., Kumar, R., and Gupta, R., Removal of malachite green dye from aqueous solution by adsorption using agro-industry waste,Dyes Pigments,vol, 62, pp, 1-10, 2004.
- [9] Perieira, M.F.R., Soares, S.F., orfao, J.J.M.,and Figueiredo, J.L.,Adsorption of Dyes on Activated Carbons:Influence of surface chemical Groups, Carbon, vol,41, pp,811- 821, 2003.
- [10] Annadurai, G., Juang ,R.,and Lee, D., Use of cellulose-based wastes for adsorption of dyes from aqueous solutions,J.Haz. Mat,vol, B92, pp, 263 – 274,2002.
- [11] Robinson, T., Chandran, B., and Nigam, P.,Removal of dyes from a synthetic textile dye effluent by biosorption on apple pomace and wheat straw, Water Res, vol,36,pp, 2824-2830,2001.
- [12] Namasivayam, C., and Arasi, S.E.,Removal of Congo red from waste water by adsorption onto waste red mud, Chemosphere, vol,34(2), pp,401 – 417,1997.
- [13] Mckay, G.,and Poots, V.J.P., J.chem. Technol. Bio – tecnol., 30(1980) 279 -292.
- [14] Kumar, P.E., Studies on characteristics and Fluoride removal capacity of Jambonut Carbon. M.Phil.,Dissertation: BharathiarUniversity, Coimbatore, 1991,Tamilnadu, India.
- [15] Kumar, P.E., Perumal, V. ost Novel Adsorbent Derived from the Inflorescence of Palmyra (Borassuslabbellifer L.) Male Flowers.Nature Environment and Pollution,vol, 9 [3],pp, 513-518, 2010.
- [16] Waranusantigul, P., Kinetics of basic dyes biosorption by giant duckweed, Environ Pollu,vol,125, pp, 385-392, 2003.
- [17] Hameed, B.H.,Evaluation of papaya seeds as a novel non-conventional low-cost adsorbent for removal of methylene blue, J. of Hazard.Mater,vol,162, pp, 939, 2009.
- [18] Freundlich , H.Z., Adsorption in solution, phys. chem. 57[1906] 384.
- [19] Treybal, R.E., Mass transfer operations, second ed., McGrw Hill, NewYork[1968].
- [20] Ho, Y.S., Mckay,G.,Sorption of dye from aqueous solution by peat, Chemical Engineering Journal,vol, 70, pp,115, 1998.

## International Journal of Innovative Research in Science, Engineering and Technology

(An ISO 3297: 2007 Certified Organization)

**Vol. 4, Issue 2, February 2015**

- [21] Langmuir, I., Adsorption of gases on plane surfaces of glass, mica and platinum, Journal of American Chemical Society, vol, 57, pp, 1361, 1918.
- [22] Ferrero, F., Dye removal by low cost adsorbents: Hazelnut shells in comparison with wood saw dust, Journal of Hazardous Materials, vol, 142, pp, 144, 2007.
- [23] McKay, G., Blair, H.S., Gardner, J.R., Adsorption of dyes on chitin: 1. Equilibrium studies, Journal of Applied Polymer Science, vol, i, 27, pp, 3043, 1982.
- [24] Tempkin, M.J., Pyzhev, V., Kinetics of ammonia synthesis on promoted iron catalysts, Acta Physicochim URSS, vol, 12, pp, 217- 22, 1940.
- [25] Langergren, S., Zu theorie der so genannten adsorption geloster stoffe. Kungliga Svenska Vetenskapsakademien. Handlingar, vol, 24, No. 4, 1898.
- [26] Ho, Y.S., McKay, G., The kinetics of sorption of divalent metal ions onto sphagnum moss peat, Water Research, vol, 34, pp, 735, 2000.
- [27] Sparks, D.L., Kinetics of Reaction in pure and mixed systems in soil physical chemistry. CRC press, Boca Raton, 1986.
- [28] Weber, W.J., Morris, J.C., Kinetics of adsorption on carbon from solution, Journal of Sanitary Engineering Division, vol, 90, pp, 79, 1964.
- [29] Nandi, B.K., Goswami, A., Purkait, M.K., Adsorption characteristics of brilliant green dye on kaolin. J. Hazard. Mater. vol, 161, pp, 387-395, 2009.
- [30] Bai, X., Yuan, F.S., Zhang, T., Wang, J.X., Wang, H., Zhang, W.Z., Joint effect of Formaldehyde and xylene on mouse bone marrow cells. Journal of Environment and Health, vol, 29, No. 1, pp, 51-54, 2012.